International Journal of Applied Electromagnetics and Mechanics 23 (2006) 177–186
IOS Press

Characteristics of smart composite wing with SMA actuators and optical fiber sensors

Seung-Man Yang[1], Jae-Hung Han[2] and In Lee[3]
Korea Advanced Institute of Science and Technology, Daejeon 305-701, Korea
Tel.: +82 42 869 3717; E-mail: inlee@asdl.kaist.ac.kr

Abstract. Recently, morphing concepts for UAV or MAV have been significant issues in aerospace engineering. Morphing wing concept, a biomimetic technology in aerospace engineering, has been realized by various methods including changes of wing's cross-section, plan form, and spar position. This paper investigates a morphing wing with variable camber using SMA actuators. The test model is a symmetric wing structure composed of two tapered graphite/epoxy composite plates and a steel body. Shape memory alloy (SMA) is attracting much attention as actuators for controlling the shape of structures because of high recovery force and large deformation. Four pairs of the SMA wire actuators are attached on the bottom surfaces of the wings in the chord-wise direction. SMA actuators produce enough deformation to cause significant improvement the static and dynamic characteristics of the wing model. Lift and drag forces, most important static aerodynamic characteristics, were measured at various angles of attack. Lift of the wing was increased without increasing drag forces when electric current was applied to the SMA actuators. Dynamic vibration signals were measured by FBG sensor at the root of the wing. The FBG sensor was successfully applied to the monitoring of the aeroelastic unstable phenomena at various angles of attack. At flutter speed, limit cycle oscillation with constant frequency occurred. It was also observed that the vibration energy is concentrated on the flutter mode and increased with the increase of the airflow speed. The effects of the angle of attack on aeroelastic characteristics of the wing were investigated. The amplitude of the limit cycle oscillation was significantly reduced at the flutter velocity when SMA actuators were activated.

Keywords: Morphing wing, composite, biomimetic, SMA, FBG sensor

1. Introduction

Shape memory alloy (SMA) is one of the attention-getting actuators for smart structures due to two unique effects, which are known in the literature as the shape memory effect and pseudoelasticity [1]. These characteristics are resulted from phase transformations between martensite and austenite phases induced by temperature or applied stress changes. Thermal and mechanical properties of SMA present exciting design possibilities in diverse engineering fields.

There have been many studies to describe the thermo-mechanical behaviors of SMA wires with one-dimensional constitutive models. Numerical models of SMA wires proposed by Tanaka [2], Liang and Rogers [3] and Brinson and Lammering [4] are the most popular and commonly exploited ones. Zak et al. [5] experimentally validated that the Brinson model should be applied to the investigations of

[1]Senior Research Engineer, Digital Appliance Research Laboratory, LG Electronics.
[2]Assistant Professor, Department of Aerospace Engineering, KAIST.
[3]Professor, Department of Aerospace Engineering, Author for correspondence, KAIST.

1383-5416/06/$17.00 © 2006 – IOS Press and the authors. All rights reserved

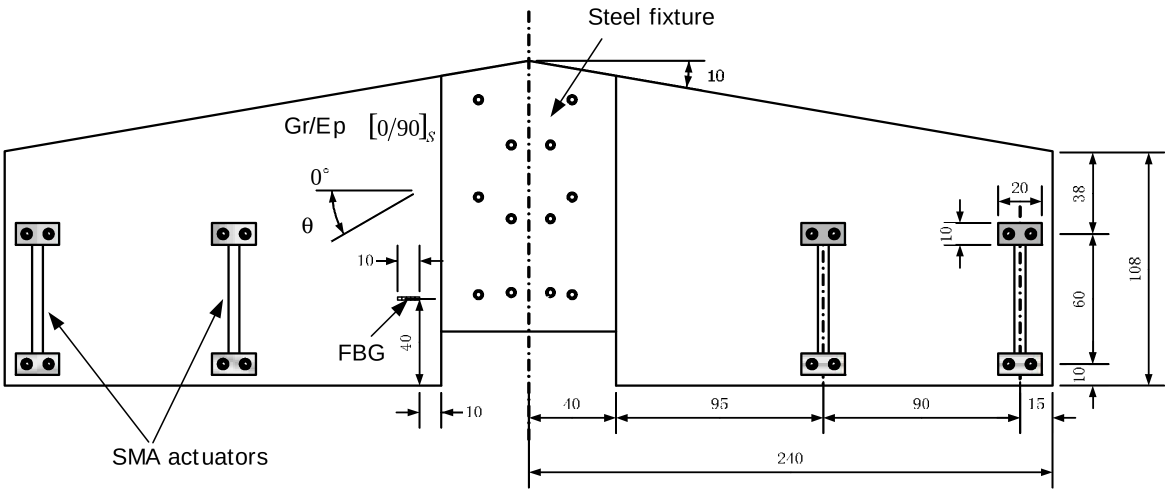

Fig. 1. Schematic diagram of Smart Composite Wing.

the shape memory and the superelastic behavior of SMA components. High recovery forces and large displacements make SMA employed in many applications such as the devices for active vibration control and shape control. Salichs et al. [6] suppressed the vibration of building structures using SMA as an energy dissipation device. Baz et al. [7] studied the active vibration control of a flexible beam using shape memory actuators. Oh et al. [8] used the SMA wires and the piezo ceramics to control the shape of parallel double plate structures. Choi and Lee [9] performed experimental and analytical studies on shape control of a flexible composite beam with embedded SMA actuators. It was shown that the SMA actuators could alter the deformed shape of composite beams that were subjected to external and thermal loads. Yang et al. [10] applied PID control algorithm to the shape control of the SMA-hybrid composite beam in order to overcome some disadvantages of the SMA actuators, such as slow response and steady state error.

Recently, morphing concepts for unmanned aerial vehicles have been significant issues in aerospace engineering [11]. Morphing structures have been realized by various methods including camber change, wing's cross-section change, and spar change [12]. SMA actuators are quite suitable for morphing wing due to its high recovery forces, large deformations and small volume. However, in order to apply SMA actuators to shape variable wings, active control should be thoroughly investigated. Most previous researches on the shape control of composite structures have been performed for the embedded SMA actuator cases. However, it is difficult to fabricate the structure with embedded SMA actuators with high reliability and electrical resistive heating for actuator activation may cause the crack in structures or debonding of SMA actuator from the structures. That is the reason why the most previous studies have focused on the numerical analysis only.

This paper investigates the aeroelastic characteristics of a Smart Composite Wing. A test model of Smart Composite Wing is fabricated to study the feasibility of the morphing using SMA actuators and improve the aerodynamic performances of the wing by chord-wise deformation. Static aerodynamics, lift and drag of the wing were observed for various electric powers applied to the SMA actuators. Using a fiber bragg grating (FBG) sensor technology [13,14], the strain signals at the root of the wing were measured with respect to fluid speeds. The flutter velocity of the wing was determined according to the spectral densities of the FBG signals. Finally, the amplitude of the limit cycle oscillation could be significantly reduced at the flutter velocity by activating the SMA actuators.

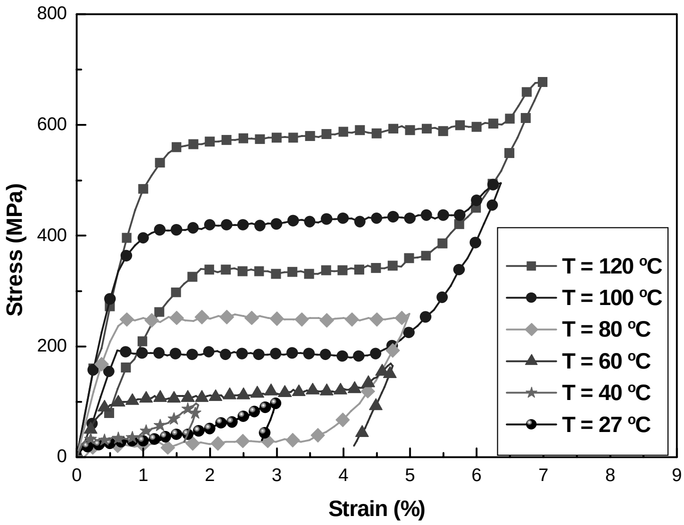

(a)

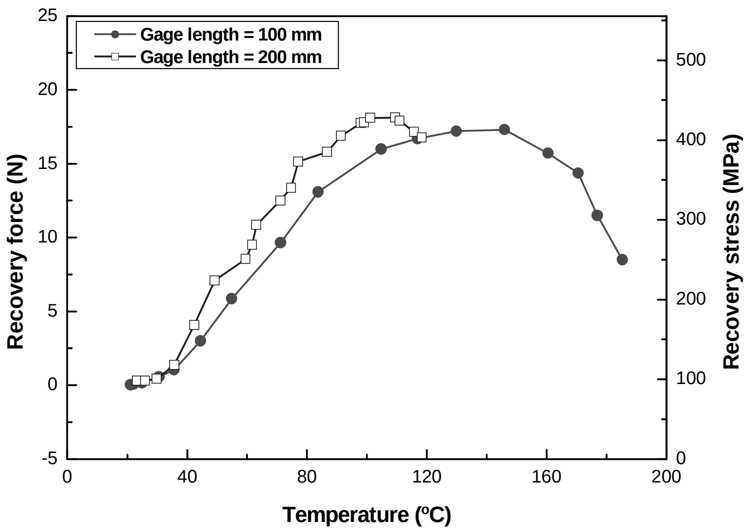

(b)

Fig. 2. Thermo-mechanical characteristics of SMA wires. (a) Stress-strain relations; (b) Recovery forces.

2. Smart composite wing

To realize the morphing wing, SMA actuators and a FBG optical fiber sensor are used with Graphite/Epoxy composite plates. The wind-tunnel test model is composed of a steel fixture, two tapered Graphite/Epoxy plates, a FBG sensor, and four pairs of SMA actuators as shown in Fig. 1. The steel center fixture clamps two composite plates and connects the model to the six component pyramidal balance which can measure the six aerodynamic forces. Each pair of SMA actuators consists of two wires in parallel and is attached to the lower surfaces of the wings using bolt joint connectors. Each set

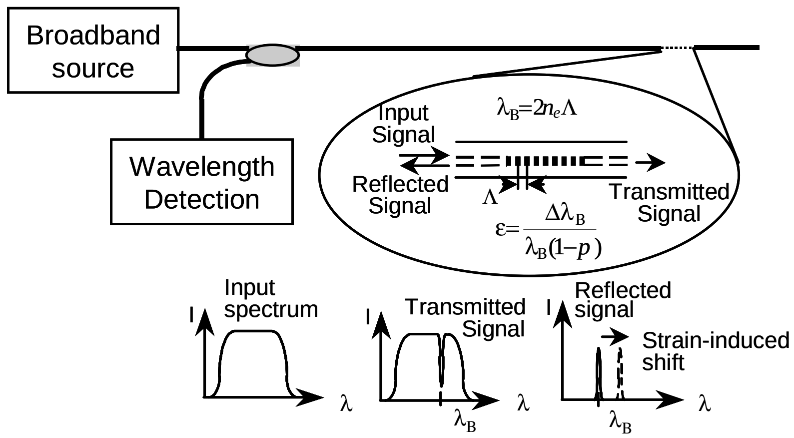

Fig. 3. FBG sensor system.

of bolt-joint connector has three brass connectors, two bolts and nuts. The FBG optical sensor is located near the root of the lower surface of the left wing.

2.1. Shape memory alloy actuators

In this research, Flexinol® manufactured by Dynalloy Inc. was selected as actuators. Flexinol® is a nickel titanium alloy and its diameter is 0.15 mm (0.006 inches). Several experiments have been performed to observe the thermo-mechanical properties of the Flexinol®. Stress-strain relations and recovery forces of the Flexinol® were measured with respect to the temperature variations as shown in Fig. 2. Loading and unloading tests at several constant temperatures were performed using INSTRON® universal testing machine 5583 and INSTRON® SFL thermal chamber. Recovery forces were measured under the fixed conditions at both ends of the SMA wires and electric powers were applied to the SMA wires to increase the temperatures. Thermocouple and load cell were used to measure the temperature and recovery forces, respectively. It was found that the SMA actuator can generate maximum 18 N forces in axial direction.

2.2. FBG optical fiber sensor

Figure 3 illustrates the basic principle of a FBG sensor, namely the measurement of Bragg wavelength shift. Therefore, it is essential to measure the Bragg wavelength shift as fast as possible in order to detect high frequency dynamics of the structure. Recently, an interrogation technique based on the wavelength-swept fiber laser (WSFL) was developed. The strain can be calculated using Eq. (1) under the constant temperature assumption.

$$\varepsilon = \frac{1}{1 - p_e} \cdot \frac{\Delta\lambda_B}{\lambda_B} \tag{1}$$

where, ε is a mechanical strain, p_e a photoelastic constant, λ_B Bragg wavelength, and $\Delta\lambda_B$ Bragg wavelength shift, respectively. In this study, WSFL (FiberPro, IS7000) is used to measure the dynamic signals.

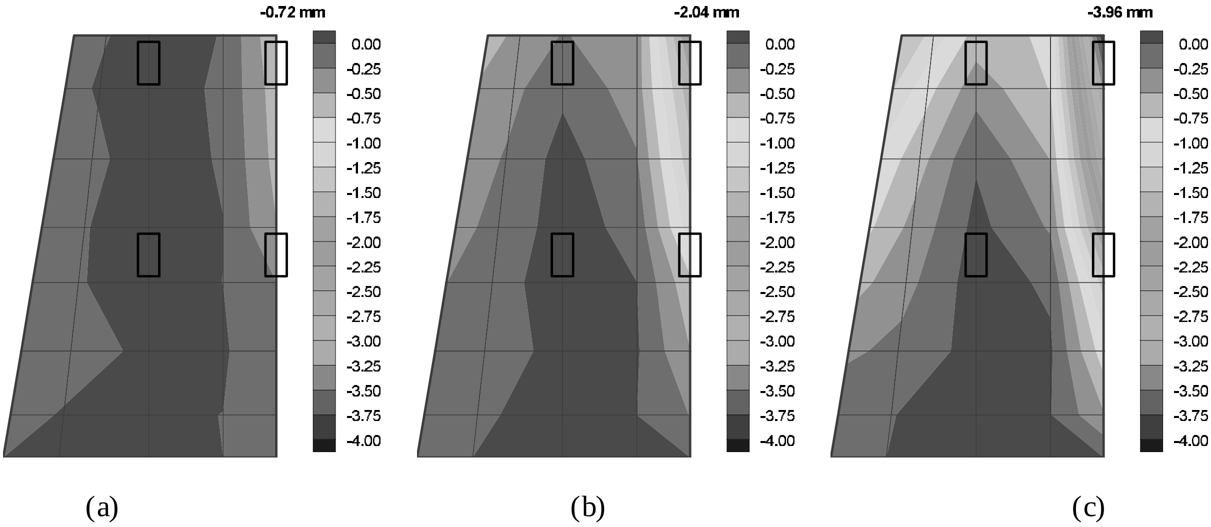

Fig. 4. Static deformations of Smart Composite Wing with respect to applied electric current. (a) 0.4 Ampere; (b) 0.5 Ampere; (c) 0.6 Ampere.

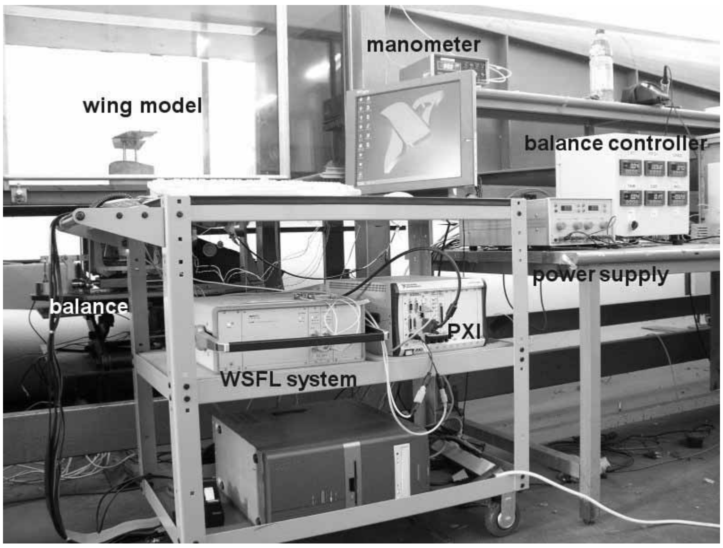

Fig. 5. Experimental setup for wind tunnel tests.

2.3. Static deformation

Static deformations of the Smart Composite Wing were measured for various applied electric powers to confirm the achievement of chord-wise deformations. Two channel high current power supply (TOELLNER, TOE8852-16) with maximum output of 160 Watt (maximum 16 Volts and 10 Amperes) per each channel was used to increase the temperature of the SMA actuators by the electric resistive heating. The deformed shapes of Smart Composite Wing are shown in Fig. 4. Maximum transverse deflections were 0.72, 2.04, and 3.96 mm when the applied currents were 0.4, 0.5, and 0.6 Amperes, respectively.

Table 1
Flutter speeds of the wing with respect to the angle of attack

Angle of attack (deg.)	Flutter speed (m/s)
0	23.1
2	18.0
4	14.9
6	14.0

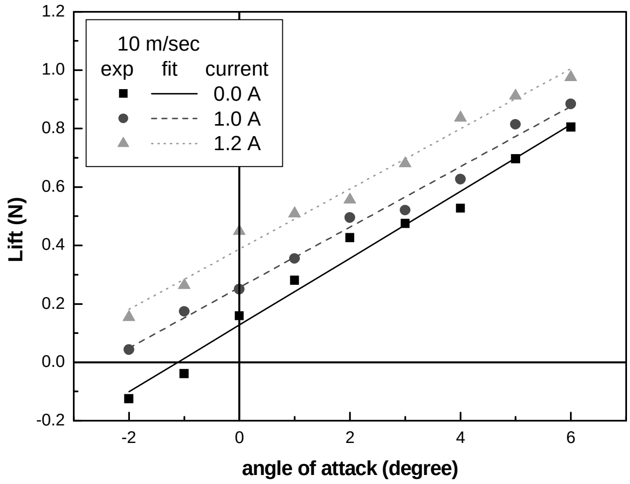

(a)

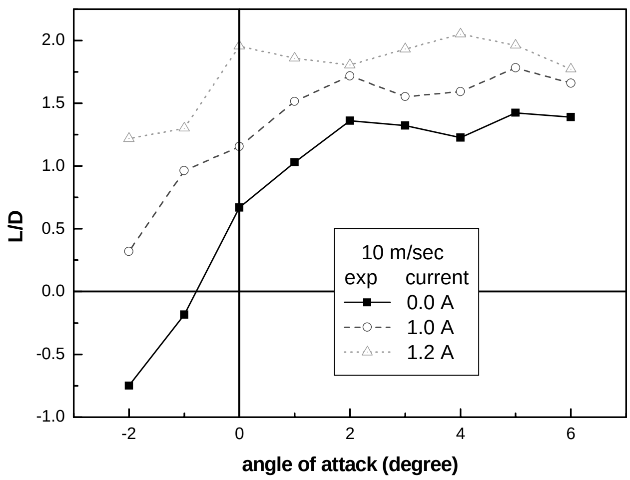

(b)

Fig. 6. Steady aerodynamics of the Smart Composite Wing with respect to the applied electric currents. (a) Lift forces; (b) L/D ratio.

3. Wind tunnel tests

The Smart Composite Wing fabricated with graphite/epoxy plate, SMA actuators, and FBG optical sensor was tested in the subsonic wind tunnel (Aerolab). Static and dynamic performances of Smart

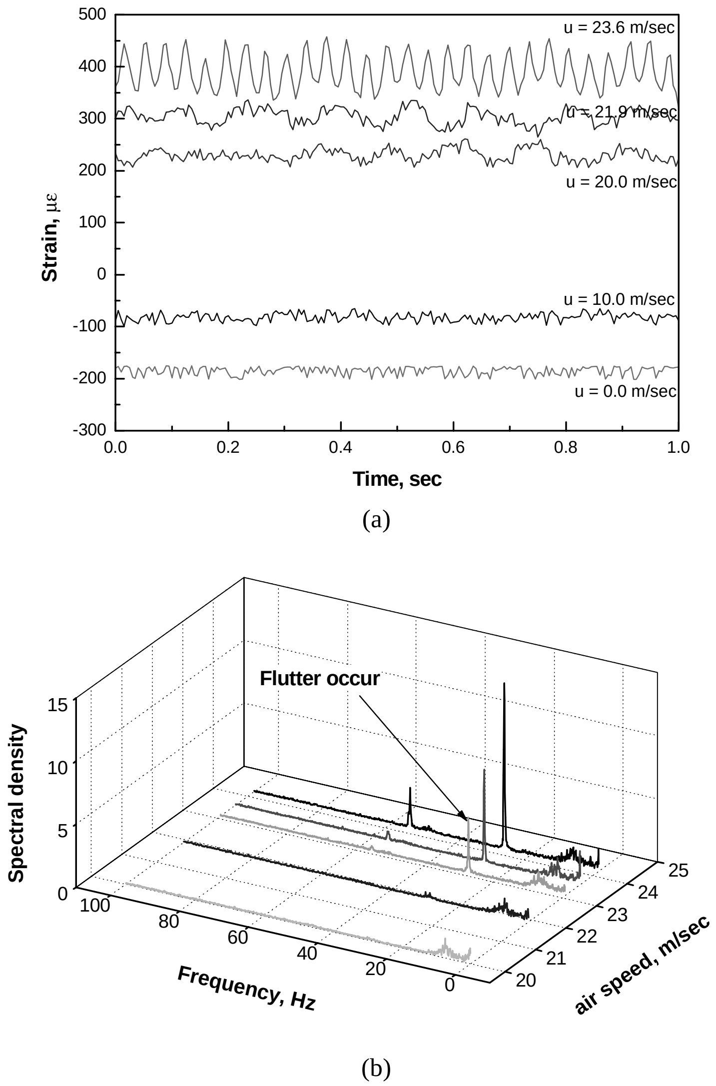

Fig. 7. FBG sensor signals of the Smart Composite Wing at various air speeds. (a) Time histories; (b) Spectral densities.

Composite Wing were measured. Overall experimental setup is shown in Fig. 5. The Smart Composite Wing was installed on the balance. In this research, six-component pyramidal balance manufactured by AeroLab in US was used to measure the steady aerodynamics. High current power supply was used to activate SMA actuators. Vibration signals of Smart Composite Wing were measured by the FBG optical sensor. Through the WSFL system, the Bragg wavelength shift was measured and data was transmitted to PXI 1042 (NI) to be stored using USB.

3.1. Steady aerodynamics

The first objective of the Smart Composite Wing is to increase the static performance of the wing using morphing concept. Static aerodynamics of the wing, Lift and Drag, were measured at constant air speed, 10.0 m/sec. Figure 6 shows the steady lift forces and lift-drag ratio of the wing with respect to the

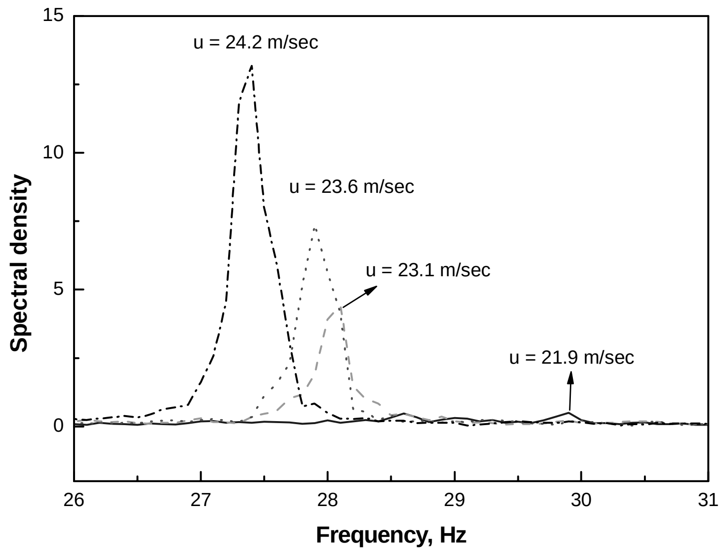

Fig. 8. Frequency shift of LCO with respect to the air flow speed.

applied electric currents to the SMA actuators. Higher electric current yielded the larger deformations of the camber lines. The Smart Composite Wing showed almost zero lift forces at -1 degrees angle of attack because of pre-deformation of the wing induced by gravity force acting on the bolt joint connector. When the wing was deformed by SMA actuators, lift is increased but drag is not much changed. From Fig. 6(b), it is found that the aerodynamic performace of Smart Composite Wing is improved when SMA actuators are activated.

3.2. Limit cycle oscillations

The second objective of this research is to investigate the flutter phenomena and the effects of the angle of attack of the wing. To measure the flutter speed of the Smart Composite Wing, strain signals were measured using the FBG sensor attached on the lower surfaces of the Wing. Figure 7(a) is the time histories of the measured strain signals at zero angle of attack. At zero airflow speed, strain is minus due to gravity force; minus strain means compression. As airflow speed is increased, the average values of the strain increased due to lift forces. At low airflow speed, small vibration was observed and when the air speed reaches 23.1 m/sec, limit cycle oscillation with constant frequency occurred. Power spectra of the strain against airflow speed are shown in Fig. 7(b). It can be found that the vibration energy is concentrated on the flutter mode and increased according to the airflow speed. The frequencies of the second peaks are twice of the first peaks. A change of the dynamic characteristics appeared when the airflow was around 23.1 m/sec, which was considered as the flutter speed. Another important phenomenon of the flutter is the changes of the modal frequencies. Figure 8 shows the close look of the power spectra around the dominant peak. The frequency of the limit cycle oscillation decreased as the airflow speed increased. This means that the flutter occurred by the merge of the second (16.2 Hz) and the third (33.4 Hz) modes of the wing structure, while the third mode was dominant. The flutter speeds at various angles of attack have been similarly determined and the results are listed in Table 1. As angle of attack increased, the flutter speed decreased.

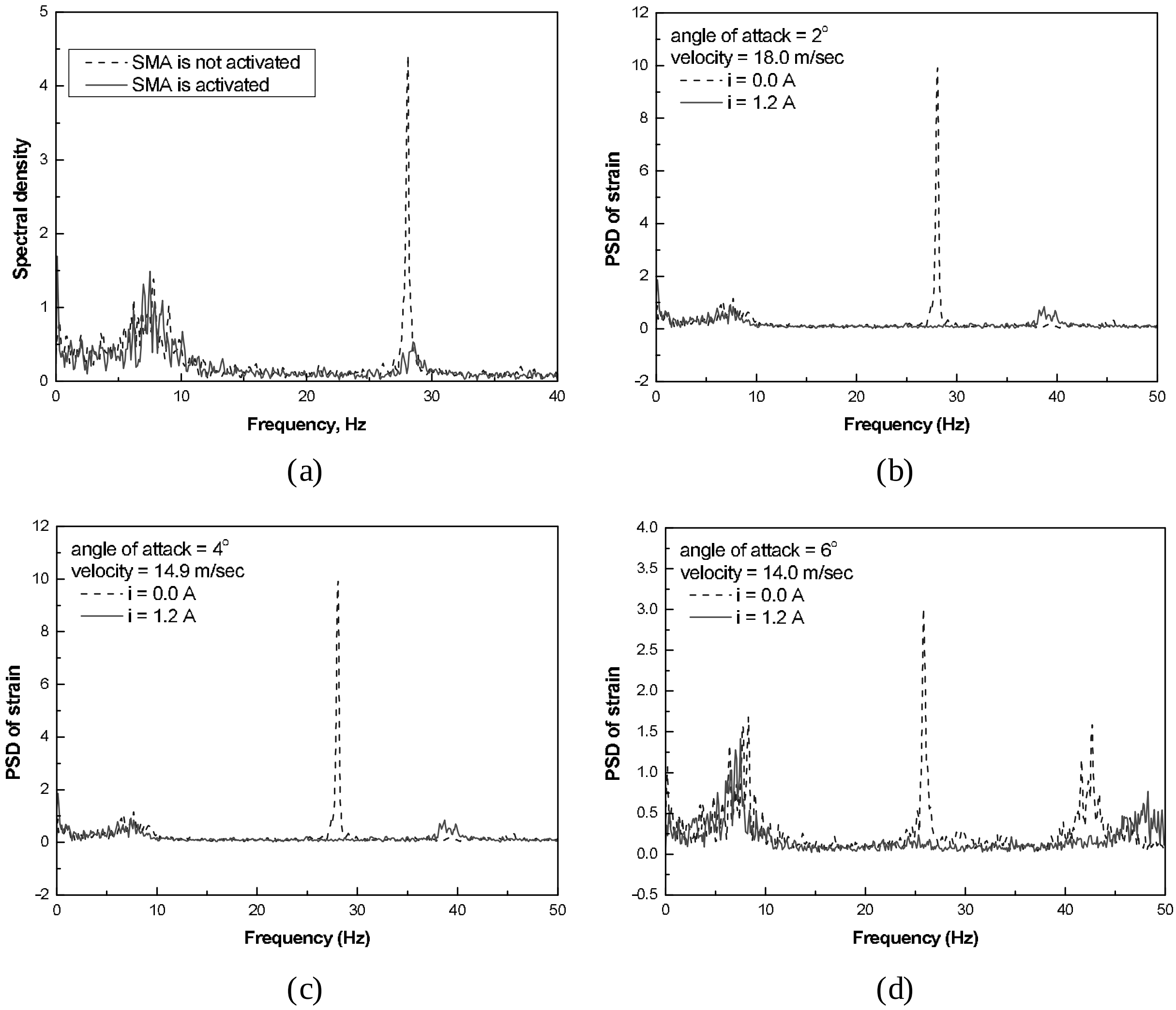

Fig. 9. Spectral densities of FBG sensor signals when SMA actuators are activated. (a) 0 degrees angle of attack; (b) 2 degrees angle of attack; (c) 4 degrees angle of attack; (d) 6 degrees angle of attack.

3.3. Stabilization of limit cycle oscillation

The third objective is to suppress the amplitude of the limit cycle oscillation induced by flutter phenomena. Generally, the modulus of shape memory alloy under austenite phase is about 2 or 3 times than martensite phase. When SMA actuators are activated by electric resistive heating, chord-wise stiffness of the Smart Composite Wing can be increased. The changes of the dynamic characteristics of the Smart Composite Wing due to SMA actuators were observed at the flutter speed. In this case, 1.2 ampere current was applied to the SMA actuators. Figure 9 shows the comparisons of the power spectra of two cases at various angles of attack. When SMA actuators were activated, the amplitude of the flutter mode was significantly reduced.

4. Conclusion

In this study, a Smart Composite Wing whose chord-wise shapes can be changed was fabricated using shape memory alloys and an FBG optical fiber sensor. Shape memory alloy actuators made enough deformation to improve the static and dynamic characteristics of the wing. The FBG sensor was successfully applied to monitoring the aeroelastically unstable phenomena. Lift of the wing was increased when electric power was applied. Flutter speeds were determined using FBG sensor signals and it was found that the angle of attack had great effects on the flutter speed. Finally, the amplitudes of the limit cycle oscillation were successfully reduced by SMA actuators at the flutter velocity. In summary, this study shows the feasibility of a Smart Composite Wing with integrated smart sensors and actuators. It is expected that this Smart Composite Wing concept can be applicable to UAV (unmanned aerial vehicle) or MAV (micro aerial vehicle) because of their relatively simple and less stiff wing structures.

Acknowledgments

This research was performed for the Smart UAV Development program, one of the 21st Century Frontier R&D Programs funded by the Ministry of Science and Technology of Korea. The authors also acknowledge the support from the National Research Laboratory (NRL) Program.

References

[1] K. Otsuka and C.M. Wayman, *Shape Memory Materials*, Cambridge University Press, 1998.
[2] K. Tanaka, A Thermomechanical Sketch for Shape Memory Effect: One-dimensional Tensile Behavior, *Res Mechanica* **18** (1986), 251–263.
[3] C. Liang and C.A. Rogers, One-dimensional Thermomechanical Constitutive Relations for Shape Memory Materials, *Journal of Intelligent Material Systems and Structures* **1**(2) (1990), 207–234.
[4] L.C. Brinson and R. Lammering, Finite Element Analysis of the Behavior of Shape Memory Alloys and their Applications, *International Journal of Solids and Structures* **30**(23) (1993), 3261–3280.
[5] A.J. Zak, M.P. Cartmell, W.M. Ostachowicz and M. Wiercigroch, One-Dimensional Shape Memory Alloy Models for Use with Reinforced Composite Structures, *Smart Materials and Structures* **12**(3) (2003), 338–346.
[6] J. Salichs, Z. Hou and M. Noori, Vibration Control of Structures Using Passive Shape Memory Alloy Energy Dissipation Devices, *Journal of Intelligent Material System and Structures* **12**(10) (2001), 671–680.
[7] A. Baz, K. Imam and J. McCoy, Active Vibration Control of Flexible Beams using Shape Memory Actuators, *Journal of Sound and Vibration* **140**(3) (1990), 437–456.
[8] J.T. Oh, H.C. Park and W. Hwang, Active Shape Control of a Double-plate Structures using Piezoceramics and SMA wires, *Smart Materials and Structures* **10**(5) (2001), 1100–1106.
[9] S. Choi and J.J. Lee, The Shape Control of a Composite Beam with Embedded Shape Memory Alloy Wire Actuators, *Smart Materials and Structures* **7**(6) (1998), 29–38.
[10] S.M. Yang, J.H. Roh, J.H. Han and I. Lee, *Numerical and Experimental Studies on Shape Tuning of Composite Plate Using SMA Actuators*, Proceedings of the Symposium on Smart materials for Engineering and Biomedical Applications, Suzhou, China, 2004, 7–14.
[11] J. Bowman, M.B. Sanders and T. Weisshaar, Evaluation of the Impact of Morphing Technologies on Aircraft Performance, AIAA SDM Paper 2002-1631, 2002.
[12] M. Amprikidis and J.E. Cooper, Development of Smart Spars for Active Aeroelastic Structures, AIAA SDM Paper 2003-1799, 2003.
[13] D.-H. Kim, J.-H. Han and I. Lee, Application of Fiber Optic Sensor and Piezoelectric Actuator to Flutter Suppression, *Journal of Aircraft* **41**(2) (2004), 409–501.
[14] D.-H. Kim, Y.-H. Chang, J.-H. Han and I. Lee, Optical Phase Estimation for a Patch-type Extrinsic Fabry-Perot Interferometer Sensor System and Its Application to Flutter Suppression, *Smart Materials and Structures* **14**(4) (2005), 696–706.